

# A Temporally and Spatially Local Spike-based Backpropagation Algorithm to Enable Training in Hardware

Anmol Biswas<sup>1</sup>, Vivek Saraswat, Udayan Ganguly

*Electrical Engineering Dept., Indian Institute of Technology, Bombay*

---

## Abstract

Spiking Neural Networks (SNNs) have emerged as a hardware efficient architecture for classification tasks. The penalty of spikes-based encoding has been the lack of a universal training mechanism performed entirely using spikes. There have been several attempts to adopt the powerful backpropagation (BP) technique used in non-spiking artificial neural networks (ANN): (1) SNNs can be trained by externally computed numerical gradients. (2) A major advancement towards native spike-based learning has been the use of approximate Backpropagation using spike-time dependent plasticity (STDP) with phased forward/backward passes. However, the transfer of information between such phases for gradient and weight update calculation necessitates external memory and computational access. This is a challenge for standard neuromorphic hardware implementations. In this paper, we propose a stochastic SNN based Back-Prop (SSNN-BP) algorithm that utilizes a composite neuron to simultaneously compute the forward pass activations and backward pass gradients explicitly with spikes. Although signed gradient values are a challenge for spike-based representation, we tackle this by splitting the gradient signal into positive and negative streams. The composite neuron encodes information in the form of stochastic spike-trains and converts Backpropagation weight updates into tem-

---

*Email addresses:* 194076019@iitb.ac.in (Anmol Biswas), svivek@iitb.ac.in (Vivek Saraswat), udayan@ee.iitb.ac.in (Udayan Ganguly)

<sup>1</sup>Corresponding Author

porally and spatially local STDP-like spike coincidence updates compatible with hardware-friendly Resistive Processing Units (RPU). Furthermore, we characterize the effect of discrete spike-based weight update to show that our method approaches BP ANN baseline with sufficiently long spike-trains. Finally, we show that the well-performing softmax cross-entropy loss function can be implemented through inhibitory lateral connections enforcing a Winner Take All (WTA) rule. Our SNN with a 2-layer network shows excellent generalization through comparable performance to ANNs with equivalent architecture and regularization parameters on the MNIST, Fashion-MNIST and Extended MNIST datasets. Thus, SSNN-BP enables BP compatible with purely spike-based neuromorphic hardware.

*Keywords:* Spiking Neural Networks, neuromorphic engineering, softmax cross-entropy

---

## 1. Introduction

Spiking Neural Networks have received long-standing interest due to their biological plausibility, efficiency as a result of the discrete nature of information propagation in such networks and theoretical computation power[1]. Additionally, recent developments like the appearance of event-driven neuromorphic hardware [2],[3] have led to a rise in interest in SNNs. SNNs implemented on such hardware are highly power-efficient compared to current neural networks which require GPUs to perform the matrix operations of learning and inference. Gradient backpropagation [4] is the basic algorithm that reliably tunes the weights and biases of neural networks and is responsible for neural networks becoming the foremost approach to solving pattern recognition and classification tasks. However, it is not straightforward to implement Backpropagation in Spiking Networks because Spiking Networks perform computations through discrete spike events that are essentially non-differentiable. Several approaches have been proposed to address this fundamental problem. One of the earliest approaches to attempt learning in Spiking Networks was SpikeProp [5], which

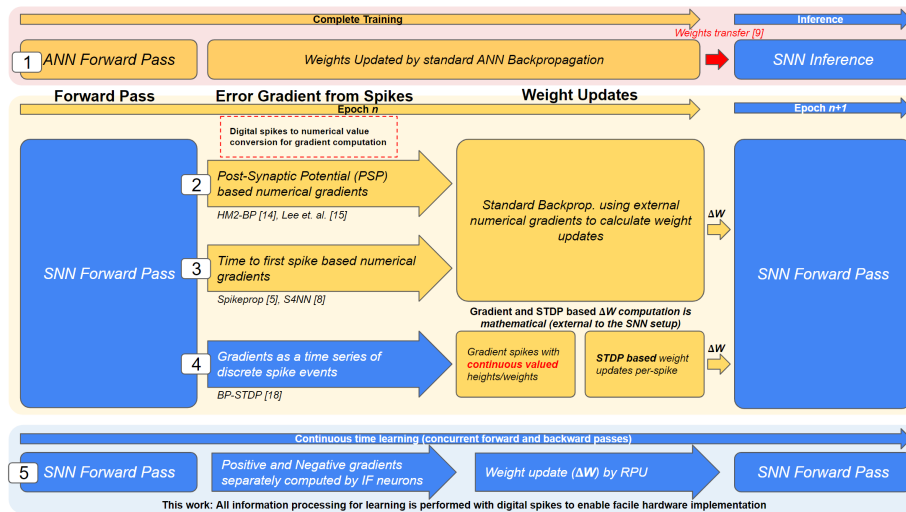


Figure 1: A comparison of the proposed algorithm with existing approaches towards learning in spiking networks. *Blue* represents purely spike-based processing while *Yellow/Orange* represents numerical processing external to the spike-based architecture. Previous work relies on generating numerical values for activations, gradients and updates in a non-spiking manner using external computation. We propose a continuous time learning where all operations in backpropagation are performed with stochastic spiking neurons.

minimized the distance between a single target and output spike by formulating the time to first spike as a function of the input to the neuron. This approach was later extended to multiple spike outputs in [6] and [7]. However, time to first spike approaches have fallen out of favor as they have been unable to compete with the performance of more recent approaches due to the weak dependence of the *time to first spike* on the input spike-train compared to the dependence of the *rate of spiking* on the same input. This holds even for the latest in time to first spike algorithms, such as S4NN[8].

An alternative and highly successful approach involves adapting trained Artificial Neural Networks (ANNs) to Spiking Networks [9],[10] and [11] where the ANN is trained separately and then the network weights are transferred to the SNN. The obvious drawback of such an approach however is that it rules out the possibility of online (or on-device) learning entirely and the training task does not benefit from the power efficient encoding that SNNs have to offer.

Finally, the third broad approach is to adapt the Backpropagation algorithm itself to rate-coded Spiking Networks. This can be done in a number of ways at various levels of complexity. In GD4SNN[12] and SLAYER[13], the instant of spiking is approximated as a continuous-time event whereas HM2-BP[14], [15] and [16] utilize exact Post-Synaptic Potentials (PSPs) to externally compute the Backpropagation gradients with high accuracy and LSNN [17] and ST-RSBP [18] utilizes Backpropagation Through Time (BPTT) with (PSPs) to train SNNs like Recurrent Neural Networks. These methods show state-of-the-art performance at classification problems using SNNs. However, one aspect common to all of these approaches is that the gradient signals need to be numerically calculated, as shown in Fig. 1, externally to the spiking network. This limits the plausible implementation of these learning algorithms in event-driven hardware because the computations involved cannot be simply translated to counting and/or timing spiking events.

In contrast, BP-STDP[19] enables spike-time dependent weight update. However, it is also a phased, serial algorithm where the backward pass is performed after the forward pass is completed and the forward pass spike trains have to be

stored externally. During the backward pass, the forward pass spike train is used to implicitly compute the loss gradient at each spike as a signed analog value externally as opposed to within the network. The weight updates occur for each pre-neuron, post-neuron spike through "approximate" STDP/Anti-STDP rules where the instantaneous gradient is used. Thus, separate forward and backward passes are used where information must be stored and transferred between the forward and backward pass phases externally. This process makes learning temporally non-local and requires significant external memory and computation.

Thus, it is an open challenge to enable temporally local updates using conventional SNN elements without requiring external memory or computation. This requires *all* the computation to be done using *only* neurons and synapses in *concurrent* forward & backward passes.

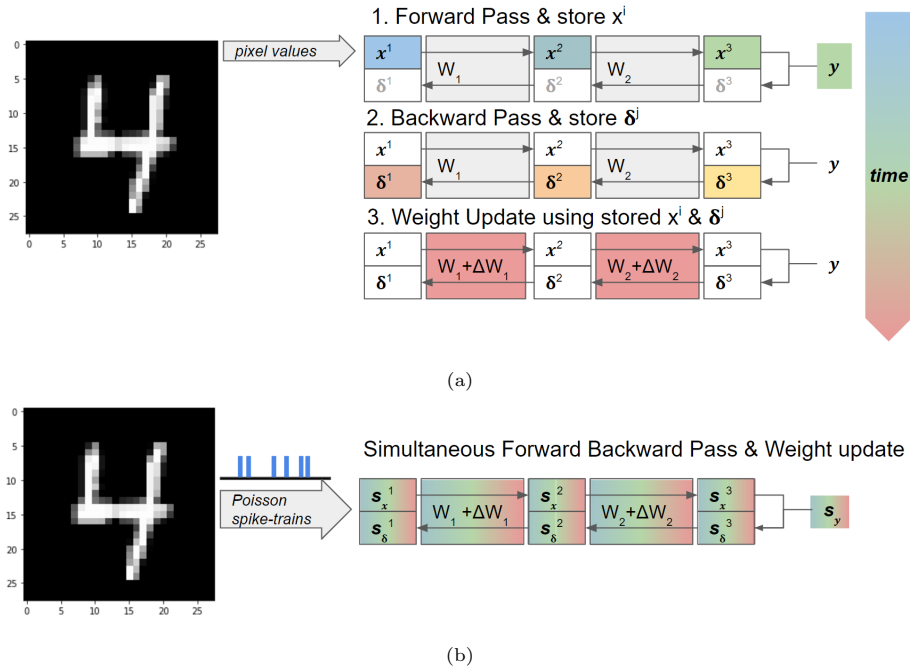


Figure 2: Network Architecture and pipeline (a) A typical serial pipeline for learning in ANNs and SNNs (b) Our learning algorithm with concurrent rate-coded computation of forward and backward passes which enables spatially and temporally local weight updates, making external storage and computations unnecessary

In this paper, we present a stochastic SNN based Back Prop (SSNN-BP), an algorithm that computes both forward-pass activations and backpropagation gradients through rate-coded spiking neurons by taking advantage of the ReLU-like[20] characteristics of Spiking Neurons, as shown in BP-STDP[19], to simplify activation and gradient relations. In contrast to BP-STDP, we split the gradient signals into positive and negative streams so that both positive and negative values can be encoded by spike-rates. Additionally, we propose lateral inhibitory connections in the output layer to implement a WTA rule[21] in order to approximate the softmax cross-entropy loss function[22]. By simultaneously generating the rate-coded forward-pass activations and backpropagation gradients, the network architecture can enable temporally and spatially local weight update rules using stochastic computing techniques devised for on-chip learning inspired by Resistive Processing Units(RPUs)[23] concept. The simultaneous forward and backward propagation ensures that no external memory is needed for learning as is the case for phased forward and backward pass with information exchange. Fig. 2 illustrates the difference between existing serial processing approaches to learning and the proposed algorithm. In our implementation, we characterize the performance degradation caused by the stochastic computation of the updates as a function of stochastic spike train duration and show the likely convergence to the performance of non-stochastic, spike-rate based backpropagation for longer pulse train duration. Finally, we benchmark the performance on SSNN-BP for different data sets i.e. MNIST, Extended MNIST and Fashion MNIST to demonstrate excellent generalization.

## 2. Proposed Method - SSNN-BP

The novel contributions of the paper can be divided into three broad elements which we describe here. First is the architecture of the network and the neuron itself. We conceptualize a composite spiking neuron that can simultaneously compute both the feedforward activations and the backpropagated gradient signals as the fundamental unit of our network. Then, we introduce

a spatially and temporally local method of generating weight updates using stochastic spike coincidence based STDP. Finally, we introduce an approximation of the softmax cross-entropy loss by using inhibitory lateral connections to enforce WTA in the output layer. For stable learning and regularization, we also adopt the He weight initialization scheme[24] and dropout[25] respectively.

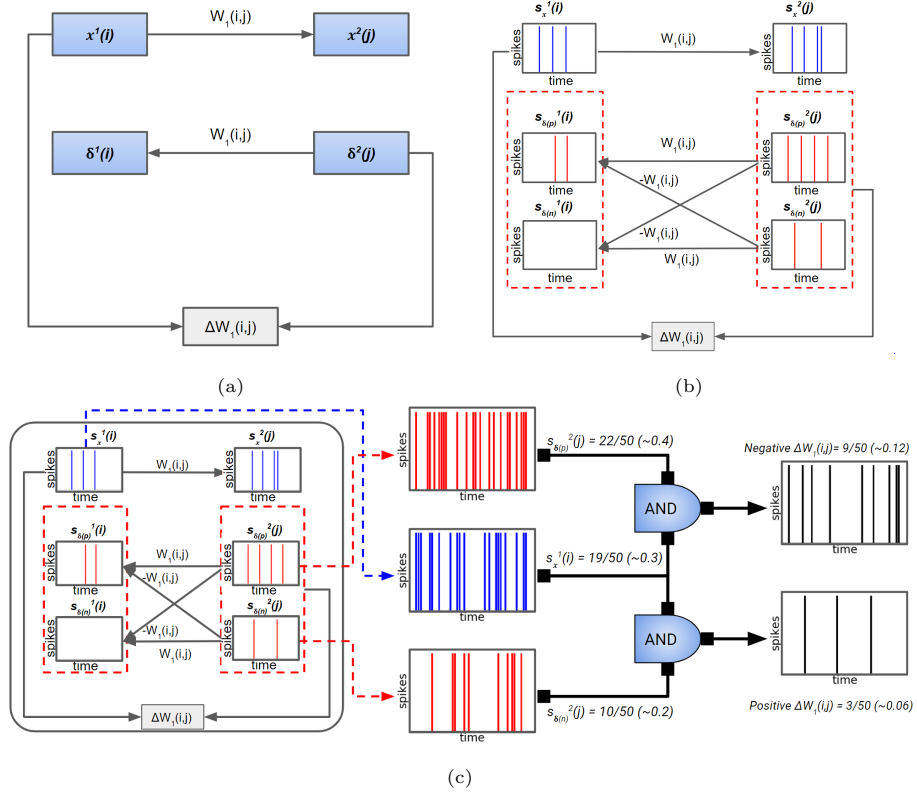


Figure 3: (a) Neuron activation, gradient and weight update computation in ANNs using real numbers (b) Example spike trains showing forward and backward passes and weight updates. The net gradient is computed as  $(s_{\delta(p)} - s_{\delta(n)})$ : this allows the representation of negative gradients with spike-rates explicitly using only spiking neurons - avoiding any implicit external computation (c) Spike-based multiplication of  $x^1(i)$  &  $\delta^2(j)$  is performed by the probability of coincidence of stochastic spike trains with *net* spike-rates  $x^1(i)$  &  $\delta^2(j)$

### 2.1. Composite Spiking Neurons

We use Integrate and Fire (IF) neurons similar to the ones described in BP-STDP[19] for our network, which we describe in terms of Spike Response Kernels as shown by the following equation :

$$s_x^{l+1} = f_{th,\theta}(\epsilon * (W_l \times s_x^l)) \quad (1)$$

$$s_x^N = f_{th,\theta}(\epsilon * (s_x^N - W_{inh} \times s_x^N)) \quad (2)$$

In Eq. 1,  $s_x^l$  represents the rate-coded spike train representation of the activations  $x$  for layer  $l$ ,  $W_l$  is the weight matrix connecting layer  $l$  to layer  $l + 1$ ,  $\epsilon$  is the Spike Response kernel,  $*$  represents convolution in time and  $f_{th}$  is the threshold function that issues spikes when the potential being computed crosses the threshold  $\theta$ . In our simulations, we set  $\theta$  to 5. The lateral inhibition in the output layer of the network is implemented by an iterative method, one iteration of which is described in Eq. 2 where all diagonal elements in  $W_{inh}$  are set to 0. We use a Spike Response kernel similar to the rising potential of an RC circuit :

$$\epsilon(t) = 1 - e^{-t/\tau} \quad (3)$$

The parameter  $\tau$  in Eq. 3 describes how fast the potential kernel value rises. This Spike Response Kernel is simply the scaled form of the time integral of a first-order synaptic current as described in HM2-BP[14]. The value of  $\tau$  is set to  $T_s/10$  where  $T_s$  is the number of simulation steps or the length of the spike train being simulated. For inference, we use  $argmax(\sum_t(s_x^N))$ . This describes the neurons for computing the feedforward spikes, we also have a set of parallel networks that compute the backpropagation losses. Two such backpropagation neurons are required for each feedforward neuron because the backpropagated gradient can be either positive or negative, while having only positive values is sufficient for feedforward neurons as shown by the success of Rectified Linear Units (ReLUs) [20], [26]. The spiking of the backpropagation neurons can be

described by the following set of equations :

$$s_{\delta(p)}^l = \left( \sum_t s_x^l > 0 \right) \otimes f_{th, \theta_b}(\epsilon * (W_l^T \times s_{\delta(p)}^{l+1} - W_l^T \times s_{\delta(n)}^{l+1})) \quad (4)$$

$$s_{\delta(n)}^l = \left( \sum_t s_x^l > 0 \right) \otimes f_{th, \theta_b}(\epsilon * (W_l^T \times s_{\delta(n)}^{l+1} - W_l^T \times s_{\delta(p)}^{l+1})) \quad (5)$$

In Eq. 4 and Eq. 5,  $s_{\delta(p)}^l$  and  $s_{\delta(n)}^l$  are the positive and negative branches of the rate-coded spike-train representation of the gradient signal backpropagated to layer  $l$  from layer  $l + 1$  and  $\otimes$  represents element-wise multiplication over the time steps of the spike-train. The term  $\sum_t s_x^l > 0$  is treated as a switch that flips when  $s_x^l$  issues its first spike. The Poisson spike train in the input layer is front-loaded to minimize the loss of the gradient signal due to this switching behavior. That is, a variable spike-rate, linearly decreasing with time is used for encoding the input value proportional to the *average spike-rate*. The equations are derived by exploiting the similarity between rate-coded IF spiking neurons and ReLUs [20]. This arrangement of one feedforward and two backpropagation neurons is given the name *Composite Spiking Neuron* because it is a complete unit which computes all the signals required for learning. The working of the composite neuron unit is visualized in Fig 3b, one forward pass neuron and two gradient neurons form one composite neuron unit. The gradient signals at the output layer  $N$  is computed by :

$$s_{\delta(p)}^N = f_{th, \theta_N}(\epsilon * (s_x^{label} - s_x^N)) \quad (6)$$

$$s_{\delta(n)}^N = f_{th, \theta_N}(\epsilon * (s_x^N - s_x^{label})) \quad (7)$$

Equations Eq. 6 and Eq. 7 implement the common form of the gradient when loss is computed either as mean-squared error or as softmax cross-entropy between  $s_x^N$  and  $s_x^{label}$ , where  $s_x^{label}$  is the target output spike train. The final gradient signal is computed by :

$$s_{\delta}^l = (s_{\delta(p)}^l - s_{\delta(n)}^l)/2, \forall l \quad (8)$$

Finally, the updates to the weight matrix are computed as the outer product of  $\sum_t s_\delta^{l+1}$  and  $\sum_t s_x^l$  in accordance with backpropagation [4] as follows:

$$\Delta W_l = \eta \times \left( \sum_t s_\delta^{l+1} \right) \times \left( \sum_t s_x^l \right)^T \quad (9)$$

where  $\eta$  is the learning rate. Eq. 9 represents the weight update as a product of the rates of two spiking neurons and this equation is the one used for the non-stochastic, spike-rate based learning simulations. Under the condition that the neuron spiking is stochastic, this update computation can be implemented by a spike co-incidence scheme as shown in Fig. 3c, effectively implementing the following equation, which describes the weight updates used in the stochastic update simulations:

$$\Delta W_l = \eta \times \sum_t ((s_\delta^{l+1}) \times (s_x^l)^T) \quad (10)$$

## 2.2. Stochastic computation of weight updates

Resistive Processing Units were proposed in [27] to perform energy-efficient ANN inference and learning. The weight update computation for Learning can be performed by a stochastic multiplication operation[23] as shown by Fig. 3c. The pre-synaptic forward pass neuron and post-synaptic gradient neurons produce stochastic spike trains  $s_x^l(i)$ ,  $s_{\delta(p)}^{l+1}(j)$  and  $s_{\delta(n)}^{l+1}(j)$  with mean firing probabilities proportional to  $x^l(i)$ ,  $\delta^{l+1}(j) \times (\delta^{l+1}(j) > 0)$  and  $-\delta^{l+1}(j) \times (\delta^{l+1}(j) < 0)$  respectively. The probability of coincidence of two spikes is given by the product of the individual firing rates and allows us to implement multiplication of pre-synaptic neuron activations with post-synaptic neuron gradients, required for the weight update, simply by **AND** functions as shown in Fig. 3c. This weight update computation is both spatially and temporally local in our Network Architecture with the Composite Neuron setup as each weight update is computed by the activity of exactly 3 nodes that can be generated simultaneously. However, being a stochastic computation means that some error is introduced by the process. The error introduced by the stochastic computation is characterized in Fig. 4 and it is found to be an additive zero-mean Gaussian

Noise, with a standard deviation that falls as  $1/\sqrt{T_s}$  with increasing simulation steps ( $T_s$ ) i.e. the duration of the stochastic spike train. This is typical for stochastic representation with a finite number of simulation steps (samples)  $T_s$ .

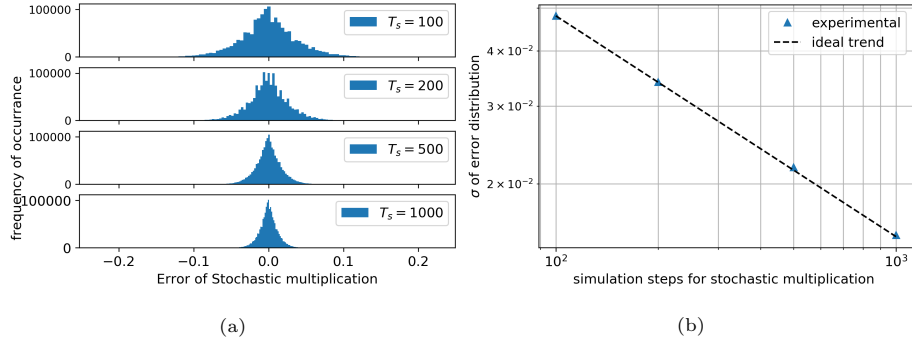


Figure 4: Characterization of the error originating from a stochastic multiplication operation. (a) Error distributions generated by computing all 2500 possible products of the array  $[0, 0.02, \dots, 0.98]$  with itself using stochastic rate-based representations for the numbers with varying number of simulation steps ( $T_s$ ) and the stochastic multiplication algorithm (b) Simulated values of the standard deviation of the error distribution generated by stochastic multiplication is plotted against the expected ideal trend

### 2.3. Softmax Cross-Entropy Loss Approximation

The softmax cross-entropy loss is an important contributing factor to improving the performance of neural networks in solving difficult classification tasks [22]. Owing to the properties of the Softmax Cross-Entropy Loss function, simply replicating a softmax-like function under a spiking paradigm is sufficient to implement learning with Softmax Cross-Entropy as the loss. However, softmax is a dynamic function that is dependent, not only on the input activation in question but also on all the other activations in the same layer. The most visible effect of the softmax function is the exaggeration of small differences between activations, where the largest activation value is enhanced and everything else is strongly suppressed by comparison. This behavior is qualitatively similar to the function of Winner Take All (WTA) networks with inhibitory lateral connections in the output layer[21].

Fig 5 compares the aggregate distribution of our WTA outputs with the corresponding softmax outputs on the same raw spiking output (without inhibitory lateral connections) over the MNIST[28] test set. After normalizing and sorting all outputs by value, the aggregate effect that the softmax function has on the distribution of output layer spiking activity is found to be very similar to the effect of WTA implemented by lateral inhibitory connections.

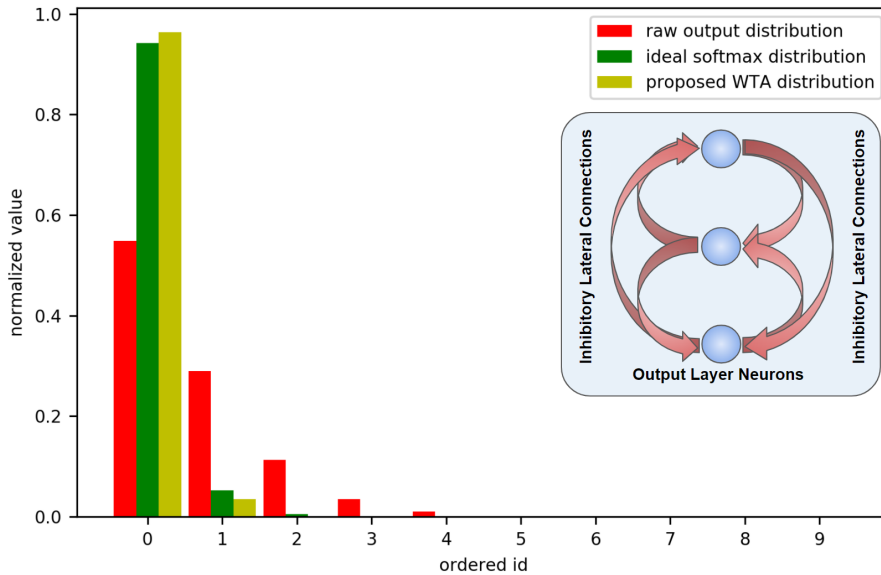


Figure 5: Comparison of the effects of softmax and WTA on the distribution of raw spiking output. Output neuron ids are sorted in descending order of response. While the raw spiking output is not so selective, WTA amplifies the nonlinearity ensuring that the primary neuron spikes uniquely while other neurons are muted. This behavior approximates the softmax function. ***Inset:*** Inhibitory lateral connections implementing WTA in output layer

### 3. Results

We test our network and supervised learning algorithm on the classification benchmark dataset - MNIST[28]. The results are compared against the state of

the art in the different approaches to learning in SNNs and ANN baseline performance. We also characterize the performance degradation introduced by the stochastic computation of weight updates, concentrating on the MNIST dataset, to estimate the optimal number of simulation steps for hardware implementation. Finally, we extend our comparison to more complex benchmark datasets - Fashion-MNIST[29] and EMNIST[30] and show generalizing capability comparable to the state of the art in SNN learning as well as the ANN baseline as well as the improvements from implementing dropout[25] and approximate softmax cross-entropy[22] loss function in our spike-based learning algorithm

Table 1: Comparison of the features and performance of learning algorithms on MNIST dataset

Model	Network	Loss and Regularizer	Gradient Computation	STDP-like weight updates	Fully SNN Compatible Learning	MNIST test-set accuracy (%)
<b>BP-STDP</b> [19]	3 layer H1=500, H2=150	MSE	<b>Discrete spikes are used to perform gradient computation and weight update for each spike but using external (non-SNN) mathematical processing</b>	Yes	No	97.2
Diehl et al. [9]	3 layer H1=1200, H2=1200	MSE	Weights are transferred from trained ANN	No	No	98.64
<b>HM2-BP</b> [14]	2 layer H1=800	MSE	Numerical gradient computation performed on continuous valued Post-Synaptic Potentials (PSPs)	No	No	<b>98.84</b>
<i>Lee et. al.</i> [15]	3 layer H1=300, H2=300	MSE and weight regularization	Numerical gradient computation performed on continuous valued Post-Synaptic Potentials (PSPs)	No	No	98.77
S4NN [8]	2 layer H1=400	MSE	Time to First Spike used for numerical gradient computation	No	No	97.4
Baseline ANN	2 layer H1=1280	softmax-CE and dropout	High precision conventional Backprop.	No	No	98.67
<b>This work</b>	<b>2 layer H1=1280</b>	<b>softmax-CE and dropout</b>	<b>Discrete spikes are used in IF neurons to implement all elements of Backprop. for learning</b>	<b>Yes</b>	<b>Yes</b>	<b>98.65 +/-0.04</b>

### 3.1. MNIST

We test the performance of the SNN and the training algorithm on the MNIST[28] handwritten numeric digit classification dataset. The dataset consists of 60,000 training samples and 10,000 test samples. Each sample is a 28x28 grayscale image. The input layer receives randomly generated Poisson spike-trains with spike-rate decreasing with time where the *average spike-rate* is set to 0.3 to 0.5 times the pixel value normalized to [0,1] and the output layer receives target Poisson spike-trains. The neuron corresponding to the correct class receives a target spike-train with a spike-rate of 0.5 while the other output layer neurons don't receive any spikes. Training the network with moderate levels of dropout (0.2 in the first layer and 0.3 in the second layer) gives test classification performance of up to 98.65%. The performance without the stochastic computation degradation is comparable to state of the art in SNNs [14],[9] as well as the ANN baseline with an equivalent architecture. Table 1 contains detailed comparisons.

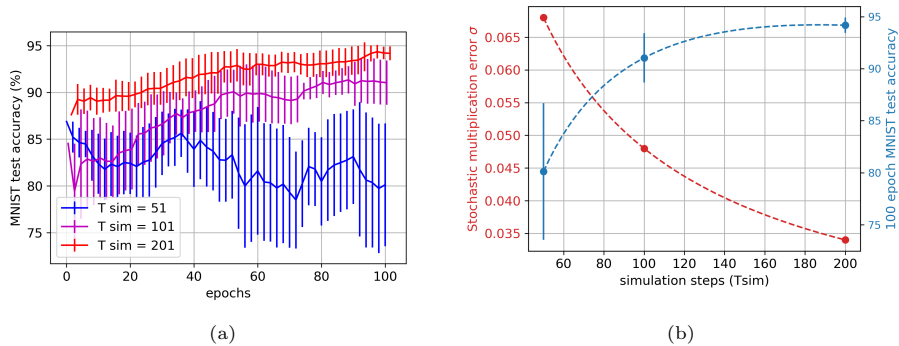


Figure 6: Learning with stochastic weight updates. **(a)** Learning with stochastic weight updates with a varying number of simulation steps. All weight updates are computed using the stochastic multiplication algorithm **(b)** The classification performance improves and stabilizes as the stochastic multiplication error falls with a larger number of simulation steps

### 3.2. Effect of Temporally local Stochastic Computation on Performance

We study the effects of the stochastic multiplication [27] algorithm for computing the weight updates for the network. The error that is introduced by

the process is characterized in Fig. 4 however, the effect of that noise on the actual performance of the network must also be studied. Fig. 6 shows the real effect of stochastic weight update computation on learning performance on the MNIST digit classification task for an increasing number of simulation steps, going from 50 to 200. There is a clear correlation between less noise and improved performance.

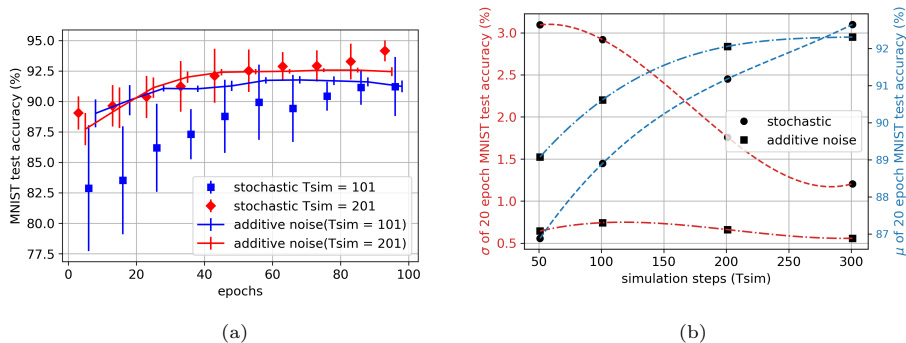


Figure 7: Comparison of learning performance (mean and variance) of pure stochastic simulations and smaller simulations with additive noise. **(a)** Comparison of learning performance of pure stochastic simulations and smaller simulations with equivalent additive noise(as characterized in Fig. 4) **(b)** Comparison of the mean and standard deviation of test accuracy after 20 epochs of learning for pure stochastic simulations and smaller simulations with equivalent additive noise

However, attempting to run anything beyond 200-step SNN simulations quickly runs up against a problem of excessive time and memory requirements. So, to estimate the long-range effects of running larger simulations, we attempt to replicate the stochastic effects by adding noise as characterized earlier in Fig. 4 onto 50-step non-stochastic (rate-based) SNN learning simulations. In Fig. 7 we validate the comparison of the pure stochastic simulations and the 50-step non-stochastic simulations with additive noise. We find that in terms of mean classification performance, the stochastic version of the learning simulations quickly catches up and seemingly overtakes the additive noise learning simulations with the increasing number of simulation steps. On the other hand, the stability (measured by the standard deviation of classification performance)

of the two types of learning simulations trend towards becoming increasingly similar.

Finally, Fig. 8 visualizes the long-range effects of increasing simulation steps by utilizing 50-step non-stochastic SNN learning simulations with additive noise to show that for large enough number of simulation steps, the performance of the stochastic multiplication based algorithm is expected to perform as well as the non-stochastic rate-based algorithm. Although, based on the trend seen in Fig. 7, the stochastic learning algorithm is likely to converge to the non-stochastic rate-based version much faster than what is predicted in Fig. 8

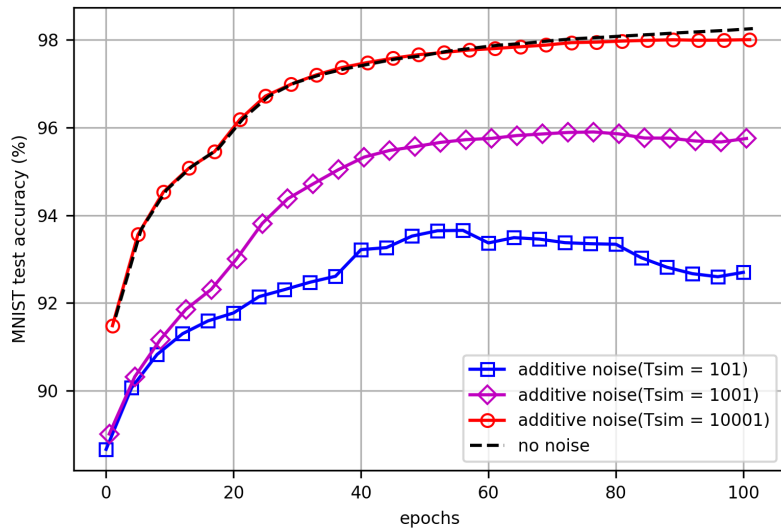


Figure 8: Learning performance of smaller simulations with additive noise for a wide range of simulation steps dependent noise levels

### 3.3. Other datasets

To showcase the generalizing property of our method, we test it on two additional datasets, *Fashion MNIST* and *Extended MNIST* which are harder classification problems than MNIST despite having identical input dimensions.

*Extended MNIST* (EMNIST) extends MNIST by adding lower and uppercase alphabets. We test our algorithm on the Balanced EMNIST dataset[30] which comprises of 131,000 labeled grayscale image samples belonging to one of 47 classes. We use 120,000 samples for training and test on 10,000 samples from the remaining. The input encoding is identical to the one described for MNIST.

*Fashion MNIST*[29] is another dataset where 28x28 grayscale images of clothing items have to be classified into 10 classes, comprising of 60,000 training and 10,000 test samples. The input encoding described for MNIST is used.

The detailed performance comparisons are provided in Table 2. Our algorithm performs better on the EMNIST and Fashion MNIST dataset compared to state of the art in SNN learning[14], [18] and approaches ANN level of performance on both datasets.

Table 2 clearly demonstrates the improvement in performance achieved by dropout regularization as well as the approximate Softmax Cross-Entropy Loss function. Adding dropout improves the test classification accuracy on the EMNIST dataset from 81.3% to 84.5% and it is further improved to 85.8% by introducing the approximate Softmax Cross-Entropy Loss.

Table 2: Generalization of SSNN-BP to EMNIST and FMNIST datasets

Model	Network	Loss and Regularizer	EMNIST test-set accuracy (%)	FMNIST test-set accuracy (%)
HM2-BP [14]	2 layer H1=800	MSE	85.41	88.99
ST-RSBP [18]	3 layer H1=400, H2=400, Recurrent Spiking Network	MSE	-	90.13
Baseline ANN	2 layer H1=1280	softmax-CE and dropout	<b>86 +/- 0.06</b>	<b>90.8 +/- 0.1</b>
This work	2 layer H1=1280	MSE	81.26 +/- 0.04	-
This work	2 layer H1=1280	MSE and dropout	84.48 +/- 0.04	-
<b>This work</b>	<b>2 layer H1=1280</b>	<b>softmax-CE and dropout</b>	<b>85.76 +/- 0.15</b>	<b>90.5 +/- 0.2</b>

### 3.4. Compatibility with Neuromorphic Hardware

The supervised training of neural networks using backpropagation of errors is a data intensive task. There has been significant thrust to transfer these operations in/near-memory and on-chip for latency and power efficient forward and

backward propagation [31]. Large neuromorphic cores of thousands of fast communicating neurons and energy efficient address event representation between hundreds of such cores have been demonstrated in digital and analog mixed mode hybrid design in hardware [32]. Chips like Neurogrid[31], TrueNorth[2], SpiNNaker[33] and Loihi[3] have made realization of very large scale neural networks possible, bringing down the time and energy complexity of network dynamics by several orders (3-4) of magnitude compared to conventional CPU and GPU simulations [32], [34].

The present trend in the neuromorphic VLSI is to increase in scale while maintaining the simplicity of individual units. Most implementations make use of simple leaky, integrate and fire neurons with methods to stochastically generate and propagate information only using spikes. These implementations also offer simple learning rules based on spike timings (STDP). The hardware acceleration benefits are not limited to just forward and backward propagation. Weight gradient calculation and weight update is another field where the role of hardware enabled efficiency is extremely critical. As described earlier, the proposal of RPU enables simultaneous calculation of gradients and write-back in large crossbar arrays of analog memories holding network weights. Since RPUs depend on generation of stochastic and pulsed representation of activations and errors, they are naturally well-suited for SNNs: spikes easily replacing the stochastic pulses needed for weight update calculation to achieve the same effect when combined with spike coincidence based learning rules. Several device level implementations of stochastic neurons using resistive memories like phase change memories [35], bulk switching PCMO RRAMs [36] and nanomagnets [37] have been proposed. Similarly, analog memories for synapses like charge trap flash [23] and DRAM-like capacitors [38] with analog charge storage have shown the feasibility of RPU. Thus algorithms tailored to a generic description of an SNN and all computations done in spikes are readily transferable and scalable on neuromorphic hardware.

#### 4. Conclusion

In this paper, we introduce a fully spike-based learning architecture for SNNs (SSNN-BP) that performs all computations using spiking neurons and performs weight updates by stochastic multiplication which implements an STDP-like spike coincidence mechanism. The algorithm is spatially and temporally local and does not require any external memory or numerical computation. We further show that its performance trends towards that of the rate-based non-stochastic version of the learning algorithm, for a large number of simulation steps, which performs on par with the state of the art in SNN learning algorithms on a number of benchmark classification tasks and approaches ANN level of performance. Furthermore, we show the performance improvement arising from introducing dropout regularization as well as adding lateral inhibitory connections in the output layer to approximate the Softmax Cross-Entropy loss function.

#### References

- [1] W. Maass, Networks of spiking neurons: the third generation of neural network models, *Neural networks* 10 (9) (1997) 1659–1671.
- [2] P. A. Merolla, J. V. Arthur, R. Alvarez-Icaza, A. S. Cassidy, J. Sawada, F. Akopyan, B. L. Jackson, N. Imam, C. Guo, Y. Nakamura, et al., A million spiking-neuron integrated circuit with a scalable communication network and interface, *Science* 345 (6197) (2014) 668–673.
- [3] M. Davies, N. Srinivasa, T.-H. Lin, G. Chinya, Y. Cao, S. H. Choday, G. Dimou, P. Joshi, N. Imam, S. Jain, et al., Loihi: A neuromorphic manycore processor with on-chip learning, *Ieee Micro* 38 (1) (2018) 82–99.
- [4] D. E. Rumelhart, G. E. Hinton, R. J. Williams, Learning representations by back-propagating errors, *nature* 323 (6088) (1986) 533–536.

- [5] S. M. Bohte, J. N. Kok, H. La Poutre, Error-backpropagation in temporally encoded networks of spiking neurons, *Neurocomputing* 48 (1-4) (2002) 17–37.
- [6] O. Booi, H. tat Nguyen, A gradient descent rule for spiking neurons emitting multiple spikes, *Information Processing Letters* 95 (6) (2005) 552–558.
- [7] S. Ghosh-Dastidar, H. Adeli, A new supervised learning algorithm for multiple spiking neural networks with application in epilepsy and seizure detection, *Neural networks* 22 (10) (2009) 1419–1431.
- [8] S. R. Kheradpisheh, T. Masquelier, Temporal backpropagation for spiking neural networks with one spike per neuron, *International Journal of Neural Systems* 30 (06) (2020) 2050027.
- [9] P. U. Diehl, D. Neil, J. Binas, M. Cook, S.-C. Liu, M. Pfeiffer, Fast-classifying, high-accuracy spiking deep networks through weight and threshold balancing, in: 2015 International joint conference on neural networks (IJCNN), iee, 2015, pp. 1–8.
- [10] P. O’Connor, D. Neil, S.-C. Liu, T. Delbruck, M. Pfeiffer, Real-time classification and sensor fusion with a spiking deep belief network, *Frontiers in neuroscience* 7 (2013) 178.
- [11] E. Hunsberger, C. Eliasmith, Spiking deep networks with lif neurons, arXiv preprint arXiv:1510.08829.
- [12] D. Huh, T. J. Sejnowski, Gradient descent for spiking neural networks, arXiv preprint arXiv:1706.04698.
- [13] S. B. Shrestha, G. Orchard, Slayer: Spike layer error reassignment in time, arXiv preprint arXiv:1810.08646.
- [14] Y. Jin, W. Zhang, P. Li, Hybrid macro/micro level backpropagation for training deep spiking neural networks, arXiv preprint arXiv:1805.07866.

- [15] J. H. Lee, T. Delbruck, M. Pfeiffer, Training deep spiking neural networks using backpropagation, *Frontiers in neuroscience* 10 (2016) 508.
- [16] C. Lee, S. S. Sarwar, P. Panda, G. Srinivasan, K. Roy, Enabling spike-based backpropagation for training deep neural network architectures, *Frontiers in neuroscience* (2020) 119.
- [17] G. Bellec, D. Sala, A. Subramoney, R. Legenstein, W. Maass, Long short-term memory and learning-to-learn in networks of spiking neurons, *arXiv preprint arXiv:1803.09574*.
- [18] W. Zhang, P. Li, Spike-train level backpropagation for training deep recurrent spiking neural networks, *Advances in neural information processing systems* 32.
- [19] A. Tavanaei, A. Maida, Bp-stdp: Approximating backpropagation using spike timing dependent plasticity, *Neurocomputing* 330 (2019) 39–47.
- [20] V. Nair, G. E. Hinton, Rectified linear units improve restricted boltzmann machines, in: *Icml*, 2010.
- [21] A. Gupta, L. N. Long, Hebbian learning with winner take all for spiking neural networks, in: *2009 International Joint Conference on Neural Networks*, IEEE, 2009, pp. 1054–1060.
- [22] P. Golik, P. Doetsch, H. Ney, Cross-entropy vs. squared error training: a theoretical and experimental comparison., in: *Interspeech*, Vol. 13, 2013, pp. 1756–1760.
- [23] V. Bhatt, S. Shrivastava, T. Chavan, U. Ganguly, Software-level accuracy using stochastic computing with charge-trap-flash based weight matrix, in: *2020 International Joint Conference on Neural Networks (IJCNN)*, IEEE, 2020, pp. 1–8.
- [24] K. He, X. Zhang, S. Ren, J. Sun, Delving deep into rectifiers: Surpassing human-level performance on imagenet classification, in: *Proceedings of the IEEE international conference on computer vision*, 2015, pp. 1026–1034.

- [25] P. Baldi, P. J. Sadowski, Understanding dropout, *Advances in neural information processing systems* 26 (2013) 2814–2822.
- [26] A. Krizhevsky, I. Sutskever, G. E. Hinton, Imagenet classification with deep convolutional neural networks, *Advances in neural information processing systems* 25 (2012) 1097–1105.
- [27] T. Gokmen, Y. Vlasov, Acceleration of deep neural network training with resistive cross-point devices: Design considerations, *Frontiers in neuroscience* 10 (2016) 333.
- [28] Y. LeCun, L. Bottou, Y. Bengio, P. Haffner, Gradient-based learning applied to document recognition, *Proceedings of the IEEE* 86 (11) (1998) 2278–2324.
- [29] H. Xiao, K. Rasul, R. Vollgraf, Fashion-mnist: a novel image dataset for benchmarking machine learning algorithms, *arXiv preprint arXiv:1708.07747*.
- [30] G. Cohen, S. Afshar, J. Tapson, A. Van Schaik, Emnist: Extending mnist to handwritten letters, in: *2017 International Joint Conference on Neural Networks (IJCNN)*, IEEE, 2017, pp. 2921–2926.
- [31] B. V. Benjamin, P. Gao, E. McQuinn, S. Choudhary, A. R. Chandrasekaran, J.-M. Bussat, R. Alvarez-Icaza, J. V. Arthur, P. A. Merolla, K. Boahen, Neurogrid: A mixed-analog-digital multichip system for large-scale neural simulations, *Proceedings of the IEEE* 102 (5) (2014) 699–716.
- [32] M. Davies, A. Wild, G. Orchard, Y. Sandamirskaya, G. A. F. Guerra, P. Joshi, P. Plank, S. R. Risbud, Advancing neuromorphic computing with loihi: A survey of results and outlook, *Proceedings of the IEEE* 109 (5) (2021) 911–934.
- [33] S. B. Furber, F. Galluppi, S. Temple, L. A. Plana, The spinnaker project, *Proceedings of the IEEE* 102 (5) (2014) 652–665.

- [34] S. Furber, Large-scale neuromorphic computing systems, *Journal of neural engineering* 13 (5) (2016) 051001.
- [35] T. Tuma, A. Pantazi, M. Le Gallo, A. Sebastian, E. Eleftheriou, Stochastic phase-change neurons, *Nature nanotechnology* 11 (8) (2016) 693–699.
- [36] D. Khilwani, V. Moghe, S. Lashkare, V. Saraswat, P. Kumbhare, M. Shojaei Baghini, S. Jandhyala, S. Subramoney, U. Ganguly, Pr x ca 1- x mno 3 based stochastic neuron for boltzmann machine to solve “maximum cut” problem, *APL Materials* 7 (9) (2019) 091112.
- [37] B. Sutton, K. Y. Camsari, B. Behin-Aein, S. Datta, Intrinsic optimization using stochastic nanomagnets, *Scientific reports* 7 (1) (2017) 1–9.
- [38] Y. Kohda, Y. Li, K. Hosokawa, S. Kim, R. Khaddam-Aljameh, Z. Ren, P. Solomon, T. Gokmen, S. Rajalingam, C. Baks, et al., Unassisted true analog neural network training chip, in: *2020 IEEE International Electron Devices Meeting (IEDM)*, IEEE, 2020, pp. 36–2.